The Journal of Veterinary Medical Science

FULL PAPER

Bacteriology

A new transformation method with nanographene oxides of antisense carrying *yycG* RNA improved antibacterial properties on methicillin-resistant *Staphylococcus aureus* biofilm

Shizhou WU[1,2], Yunjie LIU[3], Hui ZHANG[1] and Lei LEI[2]*

[1]Department of Orthopedics, West China Hospital, Sichuan University, Chengdu, 610041, China
[2]State Key Laboratory of Oral Diseases, Department of Preventive Dentistry, West China Hospital of Stomatology, Sichuan University, Chengdu, 610041, China
[3]West China School of Public Health, Sichuan University, Chengdu, 610041, China

ABSTRACT. *Staphylococcus aureus* has the potential to opportunistically cause infectious diseases. The aim of this study was to determine the antimicrobial effects of novel graphene oxide (GO)-polyethylenimine (PEI)-based antisense *yycG* (AS*yycG*) on the inhibition of methicillin-resistant *S. aureus* (MRSA) biofilm formation. In current study, a novel GO-PEI-based recombinant AS*yycG* vector transformation strategy was developed to produce AS*yycG*. The mechanical features including zeta-potential and particle size distributions were evaluated by: GO; GO-PEI and GO-PEI-AS*yycG*. The recombinant AS*yycG* vector was transformed into MRSA cells, and the expression levels of the *yycF/G* and *icaADB* genes were determined and compared by quantitative real-time PCR (qPCR) assays. The recombinant AS*yycG* plasmids were subsequently modified with a gene encoding enhanced green fluorescent protein (AS*yycG*-eGFP) as a reporter gene, and the transformation efficiency was assessed by the fluorescence intensity. The biofilm biomass and bacterial viability of the MRSA strains were evaluated by crystal violet assay, colony-forming unit assays and confocal laser scanning microscopy. The results showed that the Z-average sizes of GO-PEI-AS*yycG* were much larger than those of GO or GO-PEI. The GO-PEI-based strategy significantly increased the efficiency of AS*yycG* transformation. The GO-PEI-AS*yycG*-transformed MRSA strain had the lowest expression levels of the biofilm formation-associated genes. Furthermore, GO-PEI-AS*yycG* suppressed biofilm aggregation and improved bactericidal effects on the MRSA after 24 hr of biofilm establishment. Our findings demonstrated that GO-PEI based antisense *yycG* RNA will be an effective method for management of MRSA infections.

KEY WORDS: antisense RNA, biofilm, graphene oxide, methicillin-resistant *Staphylococcus aureus*

J. Vet. Med. Sci.
81(10): 1540–1546, 2019
doi: 10.1292/jvms.19-0216

Received: 23 April 2019
Accepted: 2 August 2019
Advanced Epub:
23 August 2019

Staphylococcus aureus is a common gram-positive cocci and coagulase-positive coccoid bacterium of the Firmicutes phylum. It has been reported that *S. aureus* forms persistent colonies in approximately 20% of healthy humans [28]. Chronic osteomyelitis is a prominent type of osteomyelitis with high recurrence rates, which may result from tenacious biofilms formed by *S. aureus*, *Streptococcus pyogenes*, *Streptococcus pneumonia*, and mycobacteria [2]. However, the extensive use of conventional antibiotics, such as penicillin, has contributed to the emergence of methicillin-resistant *S. aureus* (MRSA), resulting in significant increases in morbidity and mortality [3, 13]. In humans, MRSA is a major drug-resistant pathogen associated with a wide variety of infections from mild skin infections to life-threatening invasive diseases. Although MRSA is a significant pathogen for humans, it can also cause disease in animals [1, 14], which serve as reservoirs of MRSA that can be rapidly and repeatedly spread to humans [31].

Aggregated *S. aureus* biofilms act as virulence factors that allow MRSA strains to adhere to host organisms [8]. In biofilm formation, microbiota colonization is considered to be the critical first step for initiating the attachment and colonization of biotic surfaces by planktonic cells [10]. The microbes in the biofilm state are 1,000 times more resistant to antimicrobial agents compared to those in the planktonic state [13, 15]. Therefore, eradiation or degradation of biofilms is an essential approach for the control of biofilm-forming bacterial infections. Polysaccharide intercellular adhesion (PIA) is the key mechanism for *S. aureus* biofilm

*Correspondence to: Lei, L.: leilei@scu.edu.cn

(Supplementary material: refer to PMC https://www.ncbi.nlm.nih.gov/pmc/journals/2350/)

organization, and polysaccharides are mostly synthesized by glycosyl transferase enzymes, which are encoded by the *ica* operon [24]. PIA provides a scaffold for biofilm organization that contributes to microbial drug resistance in MRSA strains [33].

Two-component signal transduction systems (TCSs) are important in sensing and regulation mechanisms for the modulation of bacterial adaption to environmental changes [11]. Among the sixteen TCSs in *S. aureus*, YycFG is essential for bacterial viability through modulation of biofilm organization [29]. Since there is an association between the abuse of antimicrobial treatments and rising antimicrobial resistance in target bacteria, screening for supplementary therapies that lessen the use of antibiotics may be a suitable method for infection management and treatment [17, 25].

Antisense RNA is a single-stranded RNA that can specifically base-pair with its target mRNA to inhibit the transcription and translation of targeted genes [16, 18]. Our previous results indicated that antisense RNA plays a role in posttranscriptional dysregulation of target genes, resulting in a subsequent decrease in biofilm biomass [32].

AS*yycG* expresses the antisense RNA sequence of *yycG*, which is complementary to the *yycG* mRNA, and the resulting dsRNA inhibits its translation and downregulates further transcription. However, without a suitable and effective vector, the transformation efficiency of antisense oligonucleotides is limited [21]. Conventionally, a cell-penetrating peptide agent is used to facilitate the transformation process; however, the inherent toxicity and poor stability properties restricted the use of this method [12]. In recent years, graphene oxide (GO) has exhibited favorable antibacterial capacity due to its sharp edge, which can physically devastate cell membranes and induce oxidative stress reactions [35]. Indeed, new generations of GO nanocomposites that reduce bacterial adhesion to the surface of the nanomaterial surface have gained increasing attention due to their antibacterial properties [26]. Additionally, the extended surface area of the GO nanocomposites increases the capacity for carrying small molecules, such as nucleic acids, and protects them from the lysosomal degradation pathway when applied to mammalian cells [23]. In addition, the surface charge of GO can be altered by ionic bonding with a cationic polymer, such as polyethylenimine (PEI), enhancing the uptake-loading ability of biopolymers through cell membranes [36].

In the current study, we developed a graphene-based plasmid transformation system using GO-PEI complexes loaded with a *yycG* antisense expression plasmid (GO-PEI-AS*yycG*) through electrostatic interactions. The aims of this study were to (1) determine whether the transformation efficiency of the AS*yycG* gene was enhanced by the GO-PEI delivery system in the MRSA biofilm; (2) determine the antimicrobial effect of GO-PEI-AS*yycG* after transformation into an MRSA biofilm; and (3) investigate the mechanism of GO-PEI-AS*yycG* on the inhibition of MRSA biofilm formation.

MATERIALS AND METHODS

Bacterial strains and growth conditions

Ten clinically isolated MRSA strains (ST 239 type, SSC*mec* III type) were obtained from the Department of Medicine Laboratory (West China Hospital, Sichuan University, Chengdu, China). The information of those clinical isolates was listed as Supplementary Table 1. All experimental procedures were approved by their Ethical Committee (permission number 2018039A), and informed consent was obtained from the participants prior to enrollment in the study. Clinical MRSA isolates were isolated and identified from samples resected from diseased tissues, such as dead bone and medullary pus, during surgery to minimize cross contamination [6]. Briefly, the disk method was carried out to identify MRSA strains using oxacillin (1 μg) and cefoxitin (30 μg) disks. The diameters of the inhibition zones were ≤10 mm with the oxacillin disk or ≤21 mm with the cefoxitin disk. In current study, the average diameters of inhibition zones were 8.0 ± 0.5 mm for oxacillin disks and 17.5 ± 0.5 mm for cefoxitin disks. Ten MRSA clinical isolates were tested in the preliminary experiments. The results of those MRSA isolates were similar and the NO.4 strain was chosen for presenting the results in currents study. The 16S rRNA sequencing was performed to confirm the *S. aureus* strains (16S rRNA sequencing in supplementary materials). The bacteria were cultured at 37°C in tryptic soy broth (TSB) medium supplemented with 0.5% glucose and grown to mid-logarithmic growth phase (OD_{600}=0.5) for further experiments [33].

Preparation of GO-PEI-ASyycG and cytotoxicity assays

The DNA sequences coding for antisense *yycG* (AS*yycG*) were purchased as synthetic DNA from Sangon Biotech (details in the supplementary materials) and cloned into BamHI and EcoRI restriction sites in the pDL278 vector to generate the recombinant AS*yycG* pDL278 plasmids [18]. The GO-PEI complexes were produced by the addition of graphene oxide (GO) powder (XFNANO Materials Tech, Nanjing, China) into ddH_2O to a final concentration of 0.1 mg/m*l*. The solution was then mixed with the appropriate concentrations of branched polyethyleneimine (BPEI, 10 kDa; Sigma-Aldrich, St. Louis, MO, U.S.A.). To achieve complete dissolution, the mixture was sonicated on ice (ten cycles of 60 sec with 1 min intermissions), followed by gentle agitation overnight on an orbital shaker. The excess PEI was removed from the GO-PEI complex by centrifugation (12,000 × g, 1 min) and three washes with ddH_2O before resuspension with ddH_2O to a concentration of 0.1 mg/m*l*. The pDL278 AS*yycG* plasmids were dissolved in ddH_2O to a final concentration 100 *ng*/μ*l* prior to dropwise addition into the prepared GO-PEI solutions to a final ratio of 1:125 (v:v). After 1-hr incubation at room temperature, the GO-PEI-ASyycG complex was formed and further investigated [5, 7].

The optimal concentration of GO-PEI-AS*yycG* for transfection was determined by cytotoxicity assays [34]. Briefly, 3T3 fibroblast cell lines were cultured in 96-well plates (Nest Biotechnology, Wuxi, Jiangsu, China) with 100 microliters of Dulbecco Modified Eagle Medium (DMEM) to a density of 1,000 cells/well. After 48 to 72 hr of coculture with decreasing concentrations of GO-PEI-AS*yycG*, from 100 μg/m*l* to 0 μg/m*l* (37°C, 5% CO_2), the culture medium was discarded, and the wells were rinsed twice with phosphate buffer solution (PBS, pH=7.4). Cell viability was tested using a cell counting kit (CCK−8; Dojindo Laboratories, Kumamoto, Japan). After an additional 2 hr incubation, the OD values of each well were detected using a microplate reader

(ELX800, Gene, Hong Kong, China) at 540 nm.

Particle size distribution, zeta potential and atomic force microscopy measurements

The particle size distribution and the zeta-potential of GO, GO-PEI and GO-PEI-AS*yycG* solutions (0.1 mg/m*l*) were measured using a Malvern instrument (Zetasizer Malvern Nano ZS, Instruments, Worcestershire, U.K.). The GO, GO-PEI and GO-PEI-AS*yycG* films were created by dropping working solutions (50 *µl*/drop) onto sterile coverslips, which were then dried at room temperature. The roughness of the resulting films was evaluated by atomic force microscopy (AFM; SPM-9500J2, Shimadzu, Tokyo, Japan) in contact mode.

Bacterial biofilm culture and transformation

A single colony of MRSA was selected from tryptose soya agar (TSA) plates and cultured in liquid TSB medium to an OD_{600} value of 0.5, representing mid-exponential growth. Two hundred and fifty microliters of the mid-exponential phase MRSA cultures were placed in 24-well polystyrene culture plates (Nest Biotechnology, Wuxi, Jiangsu, China), and a biofilm was established on glass cover slips (14 mm in diameter) (Nest Biotechnology, Wuxi, Jiangsu, China) by culturing for 24 hr. The biofilms were then washed three times with PBS buffer to remove planktonic bacteria before the addition of transformation reagents. For the GO group, 2 *µl* of GO solution (with a concentration of 50 mg/m*l* determined by cell viability assay) was added to 24 hr old MRSA biofilms. For the AS*yycG* group, 2 *µl* of recombinant pDL278 AS*yycG* plasmid was added to the MRSA biofilm according to our previous methods. For GO-PEI-AS*yycG* transformations, 2 *µl* of the GO-PEI-AS*yycG* solution, which already included 200 *n*g of AS*yycG* plasmids, was added to 24 hr MRSA biofilms. After intervention, all the MRSA biofilms were cultured at 37°C containing 5% CO_2 for an additional 24 hr and prior to further investigation [32].

Transformation efficiency of GO-PEI-ASyycG in vitro

To determine the transformation efficiency, we created an AS*yycG* plasmid that also contained a gene encoding enhanced green fluorescent protein (AS*yycG*-eGFP). The DNA coding sequence for eGFP was synthesized by Sangon Biotech and is listed in the Supplementary materials (Page 1). We transformed AS*yycG*-eGFP and GO-PEI-AS*yycG*-eGFP into 24 hr MRSA biofilms using the procedure described above. For the AS*yycG*-eGFP group, 2 *µl* of recombinant pDL278 AS*yycG*-eGFP plasmids was mixed with 24 hr MRSA biofilms and incubated for 1 hr. For the GO-PEI-AS*yycG*-eGFP group, 2 *µl* of the GO-PEI-AS*yycG* solution (50 mg/m*l*, as determined by the cell viability assay) was transformed into 24 hr MRSA biofilms and incubated for 1 hr. Confocal laser scanning microscopy (CLSM) was applied to assess the expression level of eGFP after a 1 hr coculture. The transfection efficiency was determined by comparing the green fluorescent intensity of the transformed MRSA biofilms.

Further confirmation of the AS*yycG* transformation levels and the reduction in target gene expression in all MRSA strains was obtained using a quantitative reverse-transcribed polymerase chain reaction (qRT-PCR). Briefly, total RNA was extracted from 24 hr-treated MRSA biofilms using an RNA Purification Kit (MasterPure, Epicentre, Madison, WI, U.S.A.) following the manufacturer's instructions. Primers used in this assay and listed in Supplementary Table 2 were mixed in reactions with the RT Reagent Kit (PrimeScript, Takara, Kyoto, Japan) and run in a qRT-PCR machine (LightCycler 480, Roche, Basel, Switzerland). The primers had been validated previously, and the 16S rRNA gene was used as an internal control [33].

Evaluation of S. aureus biofilms

Crystal violet (CV) assay was applied to examine the biomass of MRSA biofilms after 24 hr interventions and MRSA without interventions as a control [4]. After a 24 hr incubation period, the MRSA biofilms were washed three times with PBS solution to remove any unattached bacterial cells. As described previously, the dye bound to the biofilms was assayed after staining with 0.1% (w/v) crystal violet for 15 min followed by destaining with 1 m*l* destaining solution (ethanol/acetone=8:2). The solution was then removed to a new plate, and the $OD_{600\ nm}$ was measured with a microplate reader (ELX800, Gene) [33]. The 24 hr biofilms were established on glass disks 14 mm in diameter (Nest Biotechnology, Wuxi, Jiangsu, China). After treatment, the biofilms were harvested by ultrasonication for 15 min in 1 m*l* of PBS. To determine the number of viable cells, the colony-forming units (CFU) was measured from the resulting microbiological samples that were serially diluted from 10^{-1} to 10^{-6} in PBS and spread onto TSA agar plates before being incubated at 37°C in 5% CO_2 for 24 hr. The viable cells on each plate was counted and calculated as CFU per millimeter of PBS suspension [32].

LIVE/DEAD test for MRSA biofilm after 24 hr transformation

The proportion of viable bacterial cells in each biofilm was estimated by confocal laser scanning microscopy (CLSM, FV1000; Olympus Corp., Tokyo, Japan) at ×40 magnification 24 hr after transformation. SYTO9 dye (LIVE/DEAD Bacterial Viability Kit reagent; BacLight, Invitrogen, Grand Island, NY, U.S.A.) was used to stain the live cells, while the dead cells were stained with propidium iodide. A three-dimensional reconstruction of the biofilm was created and analyzed by Imaris 7.0.0 software (Imaris 7.0.0, Bitplane, Zurich, Switzerland). Three biological replicates were performed for each experiment [32].

Data analysis

A Bartlett's test was conducted to determine the homogeneity of variances of the data, while a Shapiro-Wilk test was conducted to determine the normal distribution of the data. One-way analysis of variance (ANOVA) was used to compare the treatment groups, followed by pairwise multiple comparisons using statistical analysis software (SPSS version 20, IBM, Armonk, NY, U.S.A.).

RESULTS

The characteristics of GO-PEI-ASyycG

The cytotoxicity of GO-PEI-AS*yycG* was assessed using a mammalian cell viability assay, which was determined by the CCK-8 kit. After either 48 hr or 72 hr coculture, the viability of 3T3 fibroblasts cells decreased significantly when the concentration of GO-PEI-AS*yycG* was greater than 50 μg/m*l* (Supplementary Fig. 1A). Dynamic light scattering (DLS) measurements were applied to investigate the size of GO, GO-PEI and GO-PEI-AS*yycG* particles in solution. For GO and GO-PEI, Z-average sizes were approximately 390 and 280 nm, respectively, much smaller than the size of GO-PEI-AS*yycG,* which was approximately 490 nm (Supplementary Fig. 1B). The surface zeta potential value of GO was found to be approximately −23.7 mV. After the addition of the cationic polymer PEI, the GO-PEI and GO-PEI-AS*yycG* complexes demonstrated positive surface charges of 19.7 mV and 41.7 mV, respectively (Supplementary Fig. 1C). The roughness of the dried films of the GO mixtures was determined by AFM, which found that the GO-PEI-AS*yycG* sample had significantly increased roughness when compared with the GO and GO-PEI films (n=10, P<0.05; Supplementary Fig. 1D).

GO-PEI-ASyycG increased ASyycG transformation efficiency and significantly reduced expressions of biofilm associated genes

Quantitatively, there was a 180% increase in GFP fluorescence in the GO-PEI-AS*yycG*-transformed biofilms when compared with the AS*yycG*-treated biofilms (n=10, P<0.05; Fig. 1A). Quantitative RT-PCR showed that the levels of transcribed AS*yycG* RNA in the AS*yycG*- and GO-PEI-AS*yycG*-treated biofilms increased significantly by 2.5 and 5.7 times, respectively, when compared to those in the untreated MRSA biofilms (n=10, P<0.05; Fig. 1B). Consistently, the *yycF* and *yycG* gene expression levels were significantly suppressed in AS*yycG*, GO and GO-PEI-AS*yycG* biofilms (n=10, P<0.05) compared with untreated biofilms. Consequently, the transcripts of the *icaA/D/B/C* genes, which are associated with PIA synthesis, were the lowest in the GO-PEI-AS*yycG* treated group (n=10, P<0.05; Fig. 1B).

GO-PEI-ASyycG inhibited cell growth and suppressed biofilm formation

The crystal violet assays determined that the OD values of the biofilm biomasses were lowest in the GO-PEI-AS*yycG*-treated strains, indicating that GO-PEI-ASyycG suppressed MRSA biofilm formation (n=10, P<0.05, Fig. 2A and 2B). In general, the GO-PEI-AS*yycG* treatment group presented the lowest CFU, indicating an increased antimicrobial effect (Fig. 2C). The average CFU in the AS*yycG* and GO groups were also significantly decreased (P<0.05, n=10) when compared with those in the untreated MRSA group. We speculate that GO-PEI alone had some bactericidal effect against *S. aureus*. A complementary CLSM experiment was used to determine the proportion of viable bacteria. This analysis revealed that all GO-treated biofilms were decreased when compared to the untreated MRSA biofilm (Fig. 3A). The average percentages of live bacteria in the AS*yycG* and GO groups were significantly decreased (P<0.05, n=10) when compared with the MRSA group, while the lowest percentage of live bacteria was detected in the GO-PEI-AS*yycG* biofilm at 30.2 ± 5.6% (n=10, P<0.05; Fig. 3B).

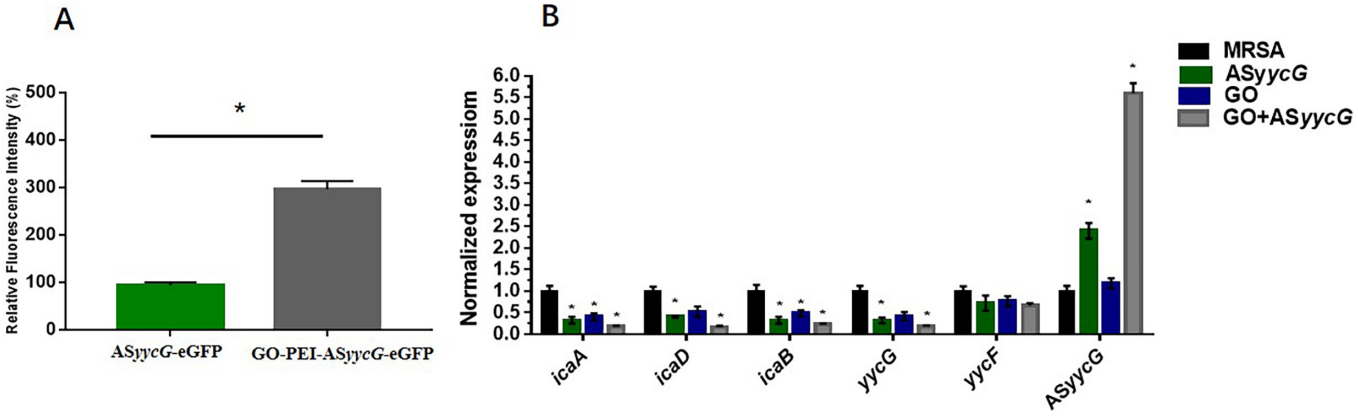

Fig. 1. GO-PEI-AS*yycG* Increased AS*yycG* transformation and inhibited virulence gene expressions. (A) The transfection efficiency was determined by comparing the green fluorescent intensities by CLSM observation (n=10, *P<0.05; GO solution with concentration at 50 mg/m*l* determined by cell viability assay); (B) Quantitative RT-PCR analysis showed gene transcription in the MRSA strains using 16S rRNA as an internal control and calculated based on the MRSA expression, which was set as 1.0. Experiments were performed in triplicate and are presented as the mean ± standard deviation (n=10, *P<0.05; GO solution with concentration at 50 mg/m*l* determined by cell viability assay). MRSA (black) indicated the control samples of MRSA cells; AS*yycG* (green) indicated the samples treated with only recombinant pDL278 AS*yycG* plasmid; GO (blue) indicated the samples treated only with GO; GO+AS*yycG* (gray) indicated the samples treated with GO+PEI based AS*yycG*. The NO.4 clinical isolated strain was used in Fig. 1.

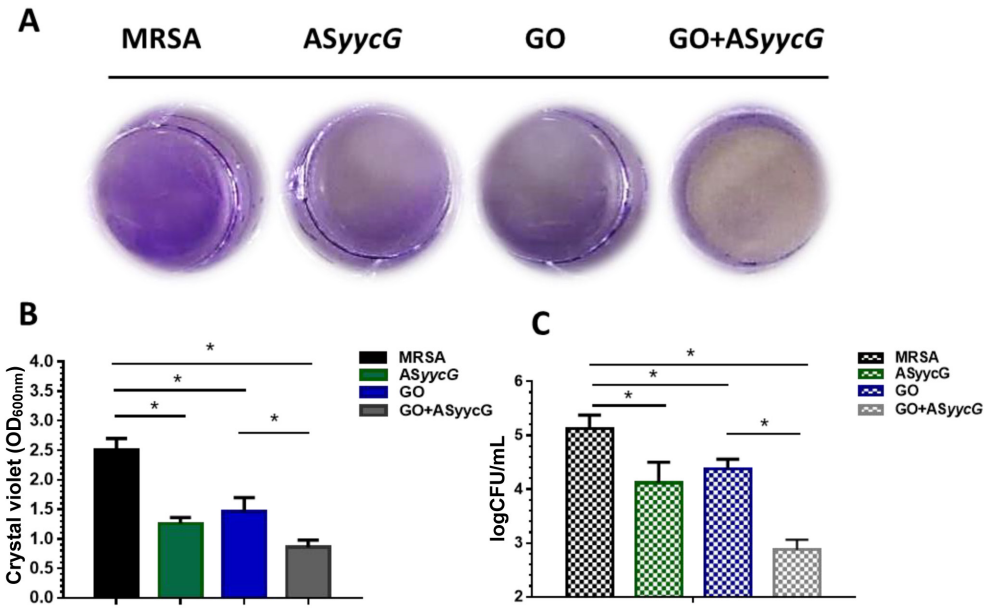

Fig. 2. GO-PEI-AS*yycG* suppressed bacterial growth and biofilm formation in MRSA biofilms. (A) Crystal violet staining for the MRSA strains; (B) Biomass was quantified by crystal violet staining; Optical densities at 600 nm were measured (n=10, **P*<0.05); (C) Colony-forming units counting for the MRSA biofilms. MRSA (black) indicated the control samples of MRSA cells; AS*yycG* (green) indicated the samples treated with only recombinant pDL278 AS*yycG* plasmid; GO (blue) indicated the samples treated only with GO; GO+AS*yycG* (gray) indicated the samples treated with GO+PEI based AS*yycG*. The NO.4 clinical isolated strain was used in Fig. 2.

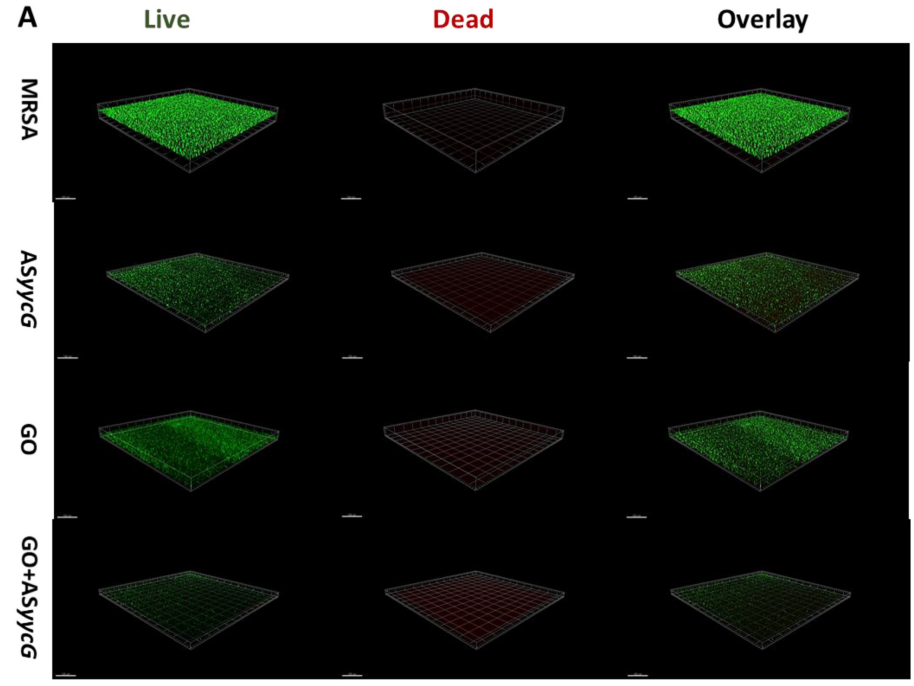

B

	MRSA	AS*yycG*	GO	GO+AS*yycG*
Live cell (%)	62.1±4.2	50.2±5.8*	53.2±6.6*	30.2±5.6*

Fig. 3. GO-PEI-AS*yycG* suppressed the vital cells in MRSA biofilms. (A) Double labeling of the biofilms in the MRSA and AS*yycG*-, GO- and GO-PEI-AS*yycG*-treated strains (GO solution with concentration at 50 mg/m*l* determined by cell viability assay). Green, vital cells (SYTO 9); red, dead cells (PI); scale bars, 100 μm; (B) Volume ratio of the vital bacterial biomass in the biofilms (n=10, **P*<0.05). The NO.4 clinical isolated strain was used in Fig. 3.

DISCUSSION

MRSA are high-priority multidrug-resistant organisms that induce serious infections in both humans and animals [30]. More effective strategies for the management of MRSA infections must be utilized to disrupt the biofilm scaffolds that are vital to infection. In the current study, we developed a GO-PEI-based strategy that showed that GO-PEI could efficiently deliver the AS*yycG* plasmid into MRSA cells and subsequently significantly inhibited the expression of *yycG*.

Cytotoxicity assays determined that concentrations of GO-PEI below 50 μg/m*l* were nontoxic, showing no cellular apoptosis [7]. In the current study, we used a 50 μg/m*l* concentration of GO-PEI-AS*yycG* composite in all experiments. When GO is ionically bound to cationic PEI polymers, the surface charges if the particles become positive, allowing the GO-PEI system to adsorb the negatively charged plasmid DNA and to interact with the negatively charged bacterial surface to promote bacterial transformation [9]. Interestingly, the GO-PEI mixtures presented smaller particle sizes than those of the GO solution. It was speculated that PEI could improve the colloidal stability of GO in aqueous solution, reducing the tendency of GO to aggregate [19]. As the surface roughness of material films could affect bacterial adhesion, it was speculated that the increased surface roughness of the GO-PEI-AS*yycG* nanosheets may provide enhanced adhesion forces.

AS*yycG* recombinant plasmids were constructed to contain a reporter gene encoding enhanced green fluorescent protein (AS*yycG*-eGFP) to evaluate the transformation efficiency of the recombinant vector. It was revealed that higher transformation efficiencies in MRSA cells were induced by GO-PEI-AS*yycG* when compared to empty AS*yycG* plasmids, as indicated by the level of fluorescence produced by GFP expression. This finding was consistent with the reduction of AS*yycG* expression transcripts as determined by quantitative RT-PCR. Graphene oxide (GO) exhibited antibacterial capacity due to its sharp edge, which can physically devastate cell membranes and induce oxidative stress reactions [35]. In present study, GO-PEI could hinder the MRSA by inhibition the biofilm formation and the expressions of YycFG pathway. It was speculated that decreased YycFG pathway transcripts would downregulate the ica associated genes [33]. The results were consistent with previous reports that the GO alone could significantly inactivate the *S. aureus* among Gram-positive and Gram-negative bacteria [20]. Also, the GO nanocomposite was capable of delivering drugs with antibacterial properties, especially for *S. aureus* [22].

In the current study, GO-PEI-AS*yycG* significantly suppressed the bacterial growth and biofilm formation of the MRSA cells (Fig. 2), and the average reduced CFU were the lowest in the GO-PEI-AS*yycG* strain, indicating that the GO-PEI-AS*yycG* treatment showed the highest antimicrobial activity. By incorporating yycG antisense-expressing plasmids into the GO-PEI complex, the GO-PEI-ASyycG particles increased the transformation of AS*yycG* into the MRSA biofilm, reducing the expression of PIA-producing enzymes and enhancing the bactericidal effects against MRSA infections. Injectable and *in situ* injectable GO-PEI-ASyycG complexes could be useful for orthopedic applications in major reconstructions of osteomyelitis lesions in humans or animals. Further *in vivo* experiments using an animal model will be needed to demonstrate the potential clinical applications and to determine the therapeutic effectiveness of the antibacterial efficacy of the GO-PEI-ASyycG construct. Hence, the applications of the GO-PEI-AS*yycG* strategy could play a potential role in managing MRSA infections even in biofilms as novel antibiotic agents. The injectable GO-PEI-ASyycG could be useful for orthopedic applications in major reconstructions of osteomyelitis lesions and reduce the use of the general glycopeptide antibiotic vancomycin [3]. Irrigation is a common procedure for clinical infection control, but the role of the treatment has been limited [27]. The GO-PEI-ASyycG at an appropriate concentration should be added with sterile saline, which could potentially improve the antibacterial properties of irrigation fluid. However, *in vivo* experiments are needed to confirm the efficiency concentration of this novel antibacterial agent before clinical application.

In summary, we have developed a novel and efficient GO-based recombinant pDL278 AS*yycG* plasmid DNA transformation strategy for the transformation of plasmid DNA into MRSA biofilms. Such transformations resulted in a reduction in the expression of the antisense gene targets and suppressed the growth of MRSA biofilms. Thus, the results demonstrated that GO-PEI-based antisense *yycG* RNA may be an effective strategy for the management of MRSA biofilm infections in both humans and animals.

CONFLICTS OF INTEREST. No conflicts of interest.

ACKNOWLEDGMENTS. We are most grateful to Huiqi Xie and Huakun Xu for their excellent technical assistance. This work was supported in part by the National Natural Science Foundation of China (Grant No. 81800964), Sichuan Provincial Natural Science Foundation of China (Grant No. 2018SZ0125 and 2019YFS0270).

REFERENCES

1. Archer, N. K., Mazaitis, M. J., Costerton, J. W., Leid, J. G., Powers, M. E. and Shirtliff, M. E. 2011. Staphylococcus aureus biofilms: properties, regulation, and roles in human disease. *Virulence* **2**: 445–459. [Medline] [CrossRef]
2. Beck-Broichsitter, B. E., Smeets, R. and Heiland, M. 2015. Current concepts in pathogenesis of acute and chronic osteomyelitis. *Curr. Opin. Infect. Dis.* **28**: 240–245. [Medline] [CrossRef]
3. Bruniera, F. R., Ferreira, F. M., Saviolli, L. R., Bacci, M. R., Feder, D., da Luz Gonçalves Pedreira, M., Sorgini Peterlini, M. A., Azzalis, L. A., Campos Junqueira, V. B. and Fonseca, F. L. 2015. The use of vancomycin with its therapeutic and adverse effects: a review. *Eur. Rev. Med. Pharmacol. Sci.* **19**: 694–700. [Medline]
4. Chen, J., Li, T., Zhou, X., Cheng, L., Huo, Y., Zou, J. and Li, Y. 2017. Characterization of the clustered regularly interspaced short palindromic repeats sites in *Streptococcus mutans* isolated from early childhood caries patients. *Arch. Oral Biol.* **83**: 174–180. [Medline] [CrossRef]
5. Dale, J. L., Cagnazzo, J., Phan, C. Q., Barnes, A. M. and Dunny, G. M. 2015. Multiple roles for Enterococcus faecalis glycosyltransferases in biofilm-

associated antibiotic resistance, cell envelope integrity, and conjugative transfer. *Antimicrob. Agents Chemother.* **59**: 4094–4105. [Medline] [CrossRef]
6. Di Bonaventura, G., D'Antonio, D., Catamo, G., Ballone, E. and Piccolomini, R. 2002. Comparison of Etest, agar dilution, broth microdilution and disk diffusion methods for testing in vitro activity of levofloxacin against Staphylococcus spp. isolated from neutropenic cancer patients. *Int. J. Antimicrob. Agents* **19**: 147–154. [Medline] [CrossRef]
7. Dou, C., Ding, N., Luo, F., Hou, T., Cao, Z., Bai, Y., Liu, C., Xu, J. and Dong, S. 2017. Graphene-Based MicroRNA Transfection Blocks Preosteoclast Fusion to Increase Bone Formation and Vascularization. *Adv Sci (Weinh)* **5**: 1700578. [Medline] [CrossRef]
8. Doulgeraki, A. I., Di Ciccio, P., Ianieri, A. and Nychas, G. E. 2017. Methicillin-resistant food-related Staphylococcus aureus: a review of current knowledge and biofilm formation for future studies and applications. *Res. Microbiol.* **168**: 1–15. [Medline] [CrossRef]
9. Feng, L., Zhang, S. and Liu, Z. 2011. Graphene based gene transfection. *Nanoscale* **3**: 1252–1257. [Medline] [CrossRef]
10. Flemming, H. C. and Wingender, J. 2010. The biofilm matrix. *Nat. Rev. Microbiol.* **8**: 623–633. [Medline] [CrossRef]
11. Fukuchi, K., Kasahara, Y., Asai, K., Kobayashi, K., Moriya, S. and Ogasawara, N. 2000. The essential two-component regulatory system encoded by yycF and yycG modulates expression of the ftsAZ operon in Bacillus subtilis. *Microbiology* **146**: 1573–1583. [Medline] [CrossRef]
12. Ghosal, A., Vitali, A., Stach, J. E. and Nielsen, P. E. 2013. Role of SbmA in the uptake of peptide nucleic acid (PNA)-peptide conjugates in E. coli. *ACS Chem. Biol.* **8**: 360–367. [Medline] [CrossRef]
13. Harkins, C. P., Pichon, B., Doumith, M., Parkhill, J., Westh, H., Tomasz, A., de Lencastre, H., Bentley, S. D., Kearns, A. M. and Holden, M. T. G. 2017. Methicillin-resistant Staphylococcus aureus emerged long before the introduction of methicillin into clinical practice. *Genome Biol.* **18**: 130. [Medline] [CrossRef]
14. Harrison, E. M., Weinert, L. A., Holden, M. T., Welch, J. J., Wilson, K., Morgan, F. J., Harris, S. R., Loeffler, A., Boag, A. K., Peacock, S. J., Paterson, G. K., Waller, A. S., Parkhill, J. and Holmes, M. A. 2014. A shared population of epidemic methicillin-resistant Staphylococcus aureus 15 circulates in humans and companion animals. *MBio* **5**: e00985–e13. [Medline] [CrossRef]
15. Ieropoli, G., Villafañe, J. H., Zompi, S. C., Morozzo, U., D'Ambrosi, R., Usuelli, F. G. and Berjano, P. 2017. Successful treatment of infected wound dehiscence after minimally invasive locking-plate osteosynthesis of tibial pilon and calcaneal fractures by plate preservation, surgical debridement and antibiotics. *Foot* **33**: 44–47. [Medline] [CrossRef]
16. Jenkins, A., Diep, B. A., Mai, T. T., Vo, N. H., Warrener, P., Suzich, J., Stover, C. K. and Sellman, B. R. 2015. Differential expression and roles of Staphylococcus aureus virulence determinants during colonization and disease. *MBio* **6**: e02272–e14. [Medline] [CrossRef]
17. Lee, A. S., de Lencastre, H., Garau, J., Kluytmans, J., Malhotra-Kumar, S., Peschel, A. and Harbarth, S. 2018. Methicillin-resistant Staphylococcus aureus. *Nat. Rev. Dis. Primers* **4**: 18033. [Medline] [CrossRef]
18. Lei, L., Stipp, R. N., Chen, T., Wu, S. Z., Hu, T. and Duncan, M. J. 2018. Activity of streptococcus mutans VicR is modulated by antisense RNA. *J. Dent. Res.* **97**: 1477–1484. [Medline] [CrossRef]
19. Liu, H., Wu, T., Wu, Z., Zhang, Y., Xuan, K., Zhang, J. and Tan, S. 2014. Poly(ethylene imine)-modified graphene oxide with improved colloidal stability and its adsorption of methyl orange. *Water Sci. Technol.* **70**: 851–857. [Medline] [CrossRef]
20. Pulingam, T., Thong, K. L., Ali, M. E., Appaturi, J. N., Dinshaw, I. J., Ong, Z. Y. and Leo, B. F. 2019. Graphene oxide exhibits differential mechanistic action towards Gram-positive and Gram-negative bacteria. *Colloids Surf. B Biointerfaces* **181**: 6–15. [Medline] [CrossRef]
21. Quijano, E., Bahal, R., Ricciardi, A., Saltzman, W. M. and Glazer, P. M. 2017. Therapeutic peptide nucleic acids: principles, limitations, and opportunities. *Yale J. Biol. Med.* **90**: 583–598. [Medline]
22. Ramezani Farani, M., Khadive Parsi, P., Riazi, G., Shafiee Ardestani, M. and Saligeh Rad, H. 2019. Extending the application of a magnetic PEG three-part drug release device on a graphene substrate for the removal of Gram-positive and Gram-negative bacteria and cancerous and pathologic cells. *Drug Des. Devel. Ther.* **13**: 1581–1591. [Medline] [CrossRef]
23. Ruiz, S., Tamayo, J. A., Ospina, J. D., Navia Porras, D. P., Valencia Zapata, M. E., Hernandez, J. H. M., Valencia, C. H., Zuluaga, F. and Grande Tovar, C. D. 2019. Antimicrobial Films Based on Nanocomposites of Chitosan/Poly(vinyl alcohol)/Graphene Oxide for Biomedical Applications. *Biomolecules* **9**: E109. [Medline] [CrossRef]
24. Rupp, M. E., Fey, P. D., Heilmann, C. and Götz, F. 2001. Characterization of the importance of Staphylococcus epidermidis autolysin and polysaccharide intercellular adhesin in the pathogenesis of intravascular catheter-associated infection in a rat model. *J. Infect. Dis.* **183**: 1038–1042. [Medline] [CrossRef]
25. Tacconelli, E., Sifakis, F., Harbarth, S., Schrijver, R., van Mourik, M., Voss, A., Sharland, M., Rajendran, N. B., Rodríguez-Baño J., EPI-Net COMBACTE-MAGNET Group 2018. Surveillance for control of antimicrobial resistance. *Lancet Infect. Dis.* **18**: e99–e106. [Medline] [CrossRef]
26. Tang, J., Chen, Q., Xu, L., Zhang, S., Feng, L., Cheng, L., Xu, H., Liu, Z. and Peng, R. 2013. Graphene oxide-silver nanocomposite as a highly effective antibacterial agent with species-specific mechanisms. *ACS Appl. Mater. Interfaces* **5**: 3867–3874. [Medline] [CrossRef]
27. Urish, K. L., Bullock, A. G., Kreger, A. M., Shah, N. B., Jeong, K., Rothenberger S. D., Infected Implant Consortium 2018. A Multicenter Study of Irrigation and Debridement in Total Knee Arthroplasty Periprosthetic Joint Infection: Treatment Failure Is High. *J. Arthroplasty* **33**: 1154–1159. [Medline] [CrossRef]
28. van Belkum, A., Verkaik, N. J., de Vogel, C. P., Boelens, H. A., Verveer, J., Nouwen, J. L., Verbrugh, H. A. and Wertheim, H. F. 2009. Reclassification of Staphylococcus aureus nasal carriage types. *J. Infect. Dis.* **199**: 1820–1826. [Medline] [CrossRef]
29. Villanueva, M., García, B., Valle, J., Rapún, B., Ruiz de Los Mozos, I., Solano, C., Martí, M., Penadés, J. R., Toledo-Arana, A. and Lasa, I. 2018. Sensory deprivation in Staphylococcus aureus. *Nat. Commun.* **9**: 523. [Medline] [CrossRef]
30. Worthing, K. A., Abraham, S., Pang, S., Coombs, G. W., Saputra, S., Jordan, D., Wong, H. S., Abraham, R. J., Trott, D. J. and Norris, J. M. 2018. Molecular characterization of methicillin-resistant staphylococcus aureus isolated from Australian animals and veterinarians. *Microb. Drug Resist.* **24**: 203–212. [Medline] [CrossRef]
31. Worthing, K. A., Brown, J., Gerber, L., Trott, D. J., Abraham, S. and Norris, J. M. 2018. Methicillin-resistant staphylococci amongst veterinary personnel, personnel-owned pets, patients and the hospital environment of two small animal veterinary hospitals. *Vet. Microbiol.* **223**: 79–85. [Medline] [CrossRef]
32. Wu, S., Liu, Y., Zhang, H. and Lei, L. 2019. The Susceptibility to Calcium Hydroxide Modulated by the Essential walR Gene Reveals the Role for Enterococcus faecalis Biofilm Aggregation. *J. Endod.* **45**: 295–301.e2. [Medline] [CrossRef]
33. Wu, S., Huang, F., Zhang, H. and Lei, L. 2019. Staphylococcus aureus biofilm organization modulated by YycFG two-component regulatory pathway. *J. Orthop. Surg.* **14**: 10. [Medline] [CrossRef]
34. Wu, S., Zhao, X., Cui, Z., Zhao, C., Wang, Y., Du, L. and Li, Y. 2014. Cytotoxicity of graphene oxide and graphene oxide loaded with doxorubicin on human multiple myeloma cells. *Int. J. Nanomedicine* **9**: 1413–1421. [Medline]
35. Yousefi, M., Dadashpour, M., Hejazi, M., Hasanzadeh, M., Behnam, B., de la Guardia, M., Shadjou, N. and Mokhtarzadeh, A. 2017. Anti-bacterial activity of graphene oxide as a new weapon nanomaterial to combat multidrug-resistance bacteria. *Mater. Sci. Eng. C* **74**: 568–581. [Medline] [CrossRef]
36. Zhang, L., Lu, Z., Zhao, Q., Huang, J., Shen, H. and Zhang, Z. 2011. Enhanced chemotherapy efficacy by sequential delivery of siRNA and anticancer drugs using PEI-grafted graphene oxide. *Small* **7**: 460–464. [Medline] [CrossRef]